 DOI: 10.5281/zenodo.13885605

EASTERN project: Earth observation models for weather event mitigation

Selene Bianco*[1], Valeria Corcione[1], Matteo Maragliano[1], Giovanna Chiara Rodi[1], Stefano Marangoni[1], Lia Morra[2], Tatiana Tommasi[2], Antonio Alliegro[2], Michelangelo Caretto[2], Rosario Milazzo[2], Osmari Aponte[3], Andrea Gatti[3], Eugenio Realini[3]

[1]*aizoOn Technology Consulting, Italy*
[2]*Politecnico di Torino, Italy*
[3]*Geomatics Research & Development (GReD), Italy*

Flooding is one of the most frequent natural disasters worldwide, resulting in substantial socioeconomic losses and public health threats. The EASTERN project proposes an innovative approach exploiting Artificial Intelligence (AI) techniques to combine data collected from Synthetic Aperture Radar (SAR) imaging and ground measurements for real-time flood risk assessment. Specifically, the goal is to focus on both immediate dangers associated with landslides and secondary risks resulting from the increased prevalence of disease vectors in affected regions. For the first use case, data from GNSS (Global Navigation Satellite System) technologies and interferometric analysis of synthetic aperture radar images (InSAR) will be combined to offer complementary insights into Earth's surface deformation and identify susceptible locations prone to landslides. For the second use case, high-resolution SAR data will be exploited to predict whether a flooded area may become an ecological niche for arbovirosis vectors. The application of advanced AI technologies for these Earth Observation tasks will allow for a prompt response to flooding events and will become a valuable support in the decision-making process of preventing and mitigating the consequences of extreme weather events.

Disclaimer This short paper is part of the project EASTERN which has received funding from Cascade funding calls of the NODES Program, supported by the MUR - M4C2 1.5 of PNRR funded by the European Union - NextGenerationEU (Grant agreement no. ECS00000036) [1].

1 Introduction

Earth observation satellites, telecommunications, global positioning systems, and scientific exploration missions are only a few among the numerous applications that provide valuable insights into the Earth's conditions and changes. Optical and radar imagery along with sensor measurements allow for the analysis of physical and meteorological factors affecting the Earth, including increasingly frequent extreme climate events, which necessitate constant monitoring to develop effective prevention and mitigation strategies.

EArth obServation models for weaThER eveNt mitigation (EASTERN) is a research project funded by the Italian Recovery and Resilience Plan through the NODES ecosystem (Digital and Sustainable North West). The aim of this project is to develop new integration and analysis models based on Artificial Intelligence (AI) (in particular Computer Vision) systems to monitor and mitigate direct and indirect impacts of extreme weather events. To this end, the characteristics of ground observation systems will be complemented by the potential of orbital observation systems. The former are precise and provide continuous time measurements but limited spatial information as they are local. On the other hand, the latter have greater geographical coverage and lower installation costs but present as their main weakness the non-continuous temporal availability.

The project's main focus is the monitoring of flooding events, including:

- direct risks caused by the event, such as landslides
- indirect risks from the flooding event, i.e. the increase in cases of the incidence of diseases carried by vectors that thrive in flooded areas.

*Corresponding author: selene.bianco@aizoongroup.com

2 Results

2.1 Use case 1 - AI-based landslide monitoring from satellite and ground data

GNSS (Global Navigation Satellite System) technologies and interferometric analysis of synthetic aperture radar images (InSAR) offer complementary insights into Earth's surface deformation [2].

In particular, InSAR combines two SAR images of the same area taken at different times to measure their difference in phase and create an interferogram, which reveals patterns indicating ground deformation or topography. For effective correlation of two SAR images, their amplitudes must be coherent, where amplitude refers to the magnitude or strength of the radar signal reflected by the Earth's surface. InSAR provides one-dimensional (1D) Line-Of-Sight (LOS) measurements on extended regions, but it is limited in determining three-dimensional (3D) displacements, and its monitoring precision may be affected by factors such as orbital and atmospheric errors.

On the other hand, GNSS is a good source of high-precision deformation monitoring data, with higher temporal resolution than InSAR (e.g. daily or hourly updates), but only for limited local regions [3]. Combining GNSS and InSAR data offers enhanced temporal coverage and improved accuracy in deformation analysis [4]. It plays an important role in disaster response and infrastructure stability monitoring applications [5].

Our objective is to develop a deep learning (DL) framework to calibrate InSAR measurements leveraging a small number of spatially-sparse GNSS measurements as a weak supervision.

The input of the deep neural network consists of InSAR measurements structured as $(N \times 9)$ point clouds. Each point of the cloud $s_i \in \mathbb{R}^9$ with $i = 1 \ldots, N$, includes three spatial (x, y, z) coordinates, and six additional parameters for ascending and descending measurements $(\theta, \alpha, D_{LOS})$. Indeed, the viewing geometry of the satellite LOS is defined by the incidence angle θ (the angle between the local zenith and the looking vector of the satellite) and the satellite heading α (see Figure 1).

The network's output is an $(N \times 3)$ array that represent an estimate of the GNSS displacements $\hat{D}_{East}, \hat{D}_{North}, \hat{D}_{Up}$ which compose $\hat{D}_{LOS}$ for each point s_i. The training supervision is provided by GNSS ground truth measurements, organized as an $(M \times 6)$ array, where M represents the number of GNSS stations and it holds $M << N$. Each station's entry includes spatial coordinates to ensure accurate mapping

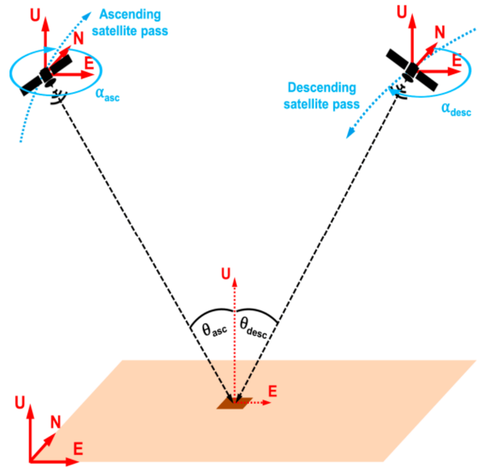

Figure 1: Schematic view of the interferometric synthetic aperture radar (InSAR) viewing geometry for Line-Of-Sight (LOS) measurements on ascending and descending satellite passes. Image source: [7]

between InSAR and GNSS data, along with ground-truth measurements for $D_{East}, D_{North}, D_{Up}$.

We implement a mapping strategy to pair each of the N network outputs with the nearest GNSS measurement. The loss function is implemented as L2-norm between the network output and the respective ground-truth measurement, where the contribution of each estimate to the overall loss is weighted inversely by the distance to its nearest GNSS measurement. This logic ensures that the closer a GNSS point is to an InSAR point, the more influence it has on the calibration of that point.

2.1.1 Data

GNSS The GNSS data set consists of seven stations along the Razdro-Vipava highway in Slovenia (refer to Figure 2), recorded under the project GIMS (Geodetic Integrated Monitoring System) [6]. The data is available from June 2019 to June 2021. For this study, the displacement data for each station was reprocessed to get a temporal resolution of one measurement per day.

InSAR We adopt InSAR data distributed by the European Ground Motion Service (EGMS). EGMS uses Sentinel-1 to provide consistent, standardized information about ground motion in European countries [8]. The initial product, known as the Basic Product (Level 2a), provides deformation velocity and deformation time series measured in the LOS direction. This product, generated using high-resolution Sentinel-1 imagery, is ideal for examining local deformation phenomena [9].

It is important to note that the temporal resolution of InSAR measurements is constrained by the satellite

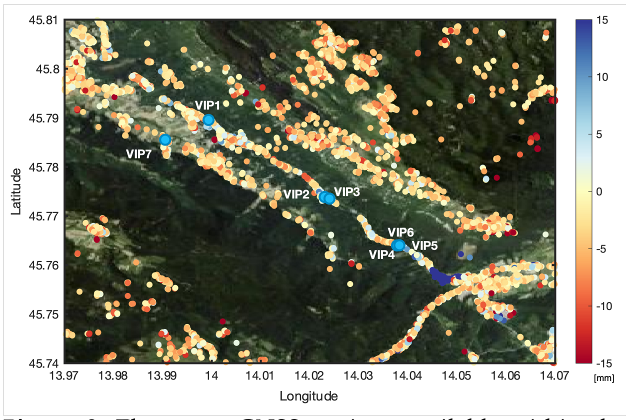

Figure 2: The seven GNSS stations available within the Razdrto-Vipava highway Area are indicated as cyan dots with their VIP label. The InSAR LOS displacements are shown in mm for the ascending orbits on February 22nd, 2021 as an example.

revisit period, which is currently six days for Sentinel-1 satellites. The data from the EGMS portal for the area of interest included three datasets for ascending orbits and two for descending orbits. These data were pre-processed for use as input in the model, combining the ascending orbits into a single dataset (refer to Figure 2). A similar procedure was applied to the descending orbits, resulting in a unified dataset for each orbit type.

2.2 Use case 2 - Flooding events - facing the spread of insect-borne infectious diseases

Vector-borne diseases make up more than 17% of infectious diseases [10] and are largely transmitted by insects. In the last two decades, the geographical areas have been expanded by the proliferation of these vectors [11]. Climate change is contributing to this expansion [12]. Therefore, it is increasingly necessary to observe weather conditions to monitor insect populations and detect epidemic precursors of diseases. Specifically, areas with pools of stagnant water are ideal for mosquitoes and other insects to proliferate [13]. Their monitoring is key to being prepared to manage emergencies that arise in flooded areas that were not previously controlled. Indeed, it is known that the spread of disease vector insects over time has a significant impact on public health [14] and can cause overloads in the healthcare system. The most efficient approaches in reducing contact between vectors and humans remain the elimination or reduction of insect populations [15] and therefore it is important to monitor and predict their movements.

To estimate in advance the dynamics of spread and mitigate the consequences on surrounding populations [16], new technologies are needed, also based on remote sensing. Correlations between the presence of reservoirs, windiness and the spread of vectors such as the Anopheles mosquito, the main vector of malaria, have been documented in the literature [17]. Satellite remote sensing can provide a wealth of information on the environmental factors that influence the abundance of vector populations, which is closely linked to the spread of the diseases they transmit [18–20] and thus enable geospatial analyses to support control and eradication programmes.

Our objective is to implement Computer Vision models that correlate the abundance of vectors in an area with certain environmental predictors (temperature, rainfall, humidity [21] and wind [17]) and with specific types of land cover [22].

In particular, the ground truth for vector estimation will be provided by ground traps, while ground cover mapping will be carried out from SAR images by fine-tuning pre-trained models [23].

Since wind is one of the key environmental factors in vector proliferation, we want to add this layer of information to the modelling. To minimise the amount of weather data needed at runtime and to allow the model to be applied in areas that are not monitored on the ground, we want to extract this information from satellite images too on flooded surfaces, as it has been done on lakes [24].

After the model has been defined to locally (geo)estimate the abundance of vectors, it would be possible to predict a risk level in a segmented area and to treat it as a risk factor in epidemiological models.

2.2.1 Data

SAR Images The dataset used for wind field retrieval from Sentinel-1 SAR images primarily relies on data from the Sentinel-1A and Sentinel-1B satellites. The Sentinel-1 mission provides various data products, which are made available systematically and free of charge to users worldwide. These products cater to both scientific and commercial needs.

Different modes of Sentinel-1 data acquisition can produce various products, including SAR Level-0, Level-1 SLC, Level-1 GRD, and Level-2 OCN. In particular, for this work, dual-pol (VV-VH) Level-1 Ground Range Detected (GRD) has been considered. GRD products are derived from detected, multi-looked, and projected SAR data onto the ground range using an Earth ellipsoid model. While these products may lose phase information, they achieve speckle reduction. The typical pixel spacing of GRD data is 10 meters, facilitating high spatial resolution.

A Sentinel-1 GRD dataset of about 500 images has been considered specifically around several Italian lakes, providing a focused geographical context for the wind field retrieval analysis. The choice of these lakes is strategic, as they represent a near-use case to flooding regions. By focusing on these lakes, which are susceptible to various environmental factors including wind dynamics, the wind field retrieval analysis can provide valuable insights that can be extrapolated to regions prone to flooding. VV-polarization has been considered due to its sensitivity to surface roughness changes induced by wind, which can be crucial for understanding and predicting wind patterns over water bodies. Wind-induced surface roughening can lead to variations in backscatter signals captured by VV-polarized SAR imagery, making it particularly relevant for studying wind dynamics over lakeshores and surrounding areas.

Metereological Data In addition to satellite imagery, meteorological data play a crucial role in wind field retrieval analysis. For this study, meteorological data have been retrieved from the Agenzia Regionale per la Protezione dell'Ambiente (ARPA) to provide with ground truth for wind speed and direction measurements.

Training Computer Vision models on Sentinel-1 SAR imagery areas that are close to meteorological stations we can improve the capabilities of wind field analysis, allowing a deeper exploration of the interactions between surface roughness, atmospheric conditions, and wind patterns.

Entomological surveillance data In response to the spread of arboviruses, i.e. viruses transmitted by blood-feeding arthropod vectors., the continuous monitoring of specific species has been enhanced in recent years by zooprophylactic and environmental monitoring institutes. Among the various mosquitoes, culex pipiens is the main vector of West Nile Virus and Usutu Virus [25]. It is of interest to this project because the biological form Cx. pipiens is predominantly rural and is more widespread in areas with little human activity, where there is non-natural water stagnation, as may be the case in rural areas impacted by flooding or in areas with stagnant crops, such as rice fields.

The available datasets concern the quantity of adult specimens captured by traps set in the monitored areas. This type of data is available on a European level [26], or by requesting access to regional zoo prophylactic institutes.

3 Discussion

The EASTERN project has an ambitious vision, which intercepts goals 3, 13 and 15 of the UN 2030 Agenda [27]. The vision is indeed to overcome and complement, through the use of AI, the ground-based observation systems by exploiting the potential of orbital observation systems, e.g. greater geographical coverage or lower cost of installation, while minimising the weaknesses of the Earth Observation systems, such as non-continuity in time.

For each of the two considered use cases, the project proposes innovative solutions. **For what concerns landslides (use case 1)**, useful strategies to integrate InSAR and GNSS data have been presented in previous works but they are either based on simplified differences among the measured displacements or leverage complex mathematical models [4, 28]. In [29] these two data types are merged through direct data fusion forming a unified deformation field. Notably, ground deformation maps have been generated at a continental scale, encompassing all of Europe in [30]. In this scenario, GNSS data were utilized to detect and eliminate potential residual atmospheric artifacts that could impact the quality of the employed MTInSAR (Multi-temporal InSAR) data. Considering the increasing adoption of integrating GNSS and SAR data for large-scale analyses, DL techniques will offer new opportunities due to their ability to handle large volumes of complex data and learn hidden patterns.

Among the indirect effects of flooding (studied in use case 2), the main objective is to train models able to predict high-resolution mapping of the risk of proliferation of vectors and their evolution over time. Defining risk by geographical area provides indications about where traps shall be installed to support monitoring and preventive measures impacts. The ecological niche of vectors like mosquitoes has been correlated with humidity, vegetation coverage, wing, and other ambiental factors [17, 31, 32]. In literature, we can find studies relating satellite imagery and weather data to predict vector populations based on trap captures [20, 33], mainly relying on vegetation, land coverage in general and moisture information [34], which can be derived from optical satellite imagery. Our approach aims to extract the predictive information from SAR images that can provide with more reliable information regardless of atmospheric conditions and have a higher penetration capability through clouds and vegetation. Moreover, SAR images are able to capture signals about wind speed for their sensitivity to water surface roughness. We expect that these advantages of SAR imagery combined with the predictive power of Computer Vision would make it easier to evaluate risks associated with specific diseases in flooded areas and be a valid support for local public health authorities in controlling outbreaks and formulating well-informed decisions.

References

1. *EASTERN. EArth obServation models for weaThER eveNt mitigation* https://www.ecs-nodes.eu/1-aerospazio-e-mobilita-sostenibile/progetti-imprese/eastern.
2. Gudmundsson, S., Sigmundsson, F. & Carstensen, J. M. Three-dimensional surface motion maps estimated from combined interferometric synthetic aperture radar and GPS data. *Journal of Geophysical Research: Solid Earth* **107,** ETG–13 (2002).
3. Bozsó, I., Bányai, L., Hooper, A., Szűcs, E. & Wesztergom, V. Integration of Sentinel-1 interferometry and GNSS networks for derivation of 3-D surface changes. *IEEE Geoscience and Remote Sensing Letters* **18,** 692–696 (2020).
4. Del Soldato, M., Confuorto, P., Bianchini, S., Sbarra, P. & Casagli, N. Review of works combining GNSS and InSAR in Europe. *Remote Sensing* **13,** 1684 (2021).
5. Crosetto, M. *et al.* The evolution of wide-area DInSAR: From regional and national services to the European Ground Motion Service. *Remote Sensing* **12,** 2043 (2020).
6. *Geodetic Integrated Monitoring System (GIMS)* https://www.gims-project.eu/.
7. Fuhrmann, T. & Garthwaite, M. C. Resolving three-dimensional surface motion with InSAR: Constraints from multi-geometry data fusion. *Remote Sensing* **11,** 241 (2019).
8. Crosetto, M., Shahbazi, S., Cuevas-González, M., Navarro, J. & Mróz, M. Advanced Analysis Tools for the European Ground Motion Service Data. *The International Archives of the Photogrammetry, Remote Sensing and Spatial Information Sciences* **48,** 1229–1234 (2023).
9. Crosetto, M. *et al. Ground Motion Examples from the European Ground Motion Service* in *IEEE IGARSS* (2022).
10. Organization, W. H. *et al. Vector-borne diseases* tech. rep. (WHO Regional Office for South-East Asia, 2014).
11. Chala, B. & Hamde, F. Emerging and re-emerging vector-borne infectious diseases and the challenges for control: a review. *Frontiers in public health* **9,** 715759 (2021).
12. Semenza, J. C. & Suk, J. E. Vector-borne diseases and climate change: a European perspective. *FEMS microbiology letters* **365,** fnx244 (2018).
13. Tusting, L. S. *et al.* Mosquito larval source management for controlling malaria. *Cochrane database of systematic reviews* (2013).
14. Guarner, J. & Hale, G. L. *Four human diseases with significant public health impact caused by mosquito-borne flaviviruses: West Nile, Zika, dengue and yellow fever* in *Seminars in diagnostic pathology* **36** (2019), 170–176.
15. Weaver, S. C., Charlier, C., Vasilakis, N. & Lecuit, M. Zika, chikungunya, and other emerging vector-borne viral diseases. *Annual review of medicine* **69,** 395–408 (2018).
16. Franklinos, L. H., Jones, K. E., Redding, D. W. & Abubakar, I. The effect of global change on mosquito-borne disease. *The Lancet infectious diseases* **19,** e302–e312 (2019).
17. Endo, N. & Eltahir, E. A. Modelling and observing the role of wind in Anopheles population dynamics around a reservoir. *Malaria Journal* **17,** 1–9 (2018).
18. Wimberly, M. C., de Beurs, K. M., Loboda, T. V. & Pan, W. K. Satellite observations and malaria: new opportunities for research and applications. *Trends in parasitology* **37,** 525–537 (2021).
19. Catry, T. *et al.* Wetlands and malaria in the Amazon: Guidelines for the use of synthetic aperture radar remote-sensing. *IJERPH* **15,** 468 (2018).
20. Field, E. N., Tokarz, R. E. & Smith, R. C. Satellite imaging and long-term mosquito surveillance implicate the influence of rapid urbanization on Culex vector populations. *Insects* **10,** 269 (2019).
21. Rosà, R. *et al.* Early warning of West Nile virus mosquito vector: climate and land use models successfully explain phenology and abundance of Culex pipiens mosquitoes in north-western Italy. *Parasites & vectors* **7,** 1–12 (2014).
22. Sallam, M. F., Al Ahmed, A. M., Abdel-Dayem, M. S. & Abdullah, M. A. Ecological niche modeling and land cover risk areas for rift valley fever vector, culex tritaeniorhynchus giles in Jazan, Saudi Arabia. *PLoS One* **8,** e65786 (2013).
23. Papoutsis, I., Bountos, N. I., Zavras, A., Michail, D. & Tryfonopoulos, C. Benchmarking and scaling of deep learning models for land cover image classification. *ISPRS* **195,** 250–268 (2023).
24. Katona, T. & Bartsch, A. Estimation of wind speed over lakes in Central Europe using spaceborne C-band SAR. *European Journal of Remote Sensing* **51,** 921–931 (2018).
25. *Piano nazionale di prevenzione, sorveglianza e risposta alle Arbovirosi (PNA) 2020-2025* 2019.
26. Á, M. C. M. & C, B. S. *AIMSurv Aedes Invasive Mosquito species harmonized surveillance in Europe. AIM-COST Action* 2022. https://ipt.gbif.es/resource?r=aimsurv (2023).
27. *2030 Agenda for Sustainable Development. The 17 goals* 2015. https://sdgs.un.org/goals.
28. Yan, H. *et al.* A method for correcting InSAR interferogram errors using GNSS data and the K-means algorithm. *Earth, Planets and Space* **76,** 51 (2024).
29. Simonetto, E. *et al.* Combination of INSAR and GNSS measurements for ground displacement monitoring. *Procedia Technology* **16,** 192–198 (2014).
30. Lanari, R. *et al.* Automatic generation of Sentinel-1 continental scale DInSAR deformation time series through an extended P-SBAS processing pipeline in a cloud computing environment. *Remote Sensing* **12,** 2961 (2020).
31. Morgan, J., Strode, C. & Salcedo-Sora, J. E. Climatic and socioeconomic factors supporting the co-circulation of dengue, Zika and chikungunya in three different ecosystems in Colombia. *PLoS Neglected Tropical Diseases* **15,** e0009259 (2021).
32. Alexander, J. *et al.* Using machine learning to understand microgeographic determinants of the Zika vector, Aedes aegypti. *PloS one* **17,** e0265472 (2022).
33. Catry, T. *et al. Fusion of SAR and optical imagery for studuing the eco-epidemiology of vector-borne diseases in tropical countries* in *European Space Agency Living Planet Symposium* (2016).
34. Wimberly, M. C., de Beurs, K. M., Loboda, T. V. & Pan, W. K. Satellite observations and malaria: new opportunities for research and applications. *Trends in parasitology* **37,** 525–537 (2021).